Chapter

Necessity of Quantitative EEG for Daily Clinical Practice

Jesús Pastor, Lorena Vega-Zelaya and Elena Martín Abad

Abstract

The two main problems in the daily clinical practice of EEG are i) its under-use dedicated mainly to epilepsy and ii) subjectivity in *de visu* analysis. However, both problems can be overcome by using numerical tools in clinical practice that broaden the scope and introduce real objectivity to bioelectrical measurements. We have developed a method for quantitative EEG (qEEG) for daily use based on the homeostatic foundation of EEG. This method is robust, easy, and not time consuming and is arranged in two branches: the analysis of the spectral composition in each channel and synchronization. Notably, channels are arranged in differential mode. Since 2016, we have used this method for more than 4100 EEGs from scalp recordings in outpatients, epilepsy evaluation, and evaluation and monitoring in the intensive care unit (ICU). We have been able to identify numerical properties that are not visually evident in several pathologies, including COVID-19 in patients suffering encephalopathy, and have performed diagnosis in ICU patients and differentiation between epileptic and non-epileptic spells or minimum cognitive states. The use of numerical variables across successive recordings in the same patient has proven to be of great utility. We propose that qEEG use should be expanded globally for daily clinical practice.

Keywords: encephalopathy, epilepsy, fast Fourier transform, numerical methods, psychogenic non-epileptic seizures, spectral entropy, synchronization

1. Introduction

Electroencephalography (EEG) is one of the oldest diagnostic methods currently used in medicine. It was described one century ago by the German psychiatrist Hans Berger [1]. Since then, its use has rapidly spread, and practically every hospital in the world has an EEG device. However, although EEG is probably the fastest, cheapest, and most straightforward method to obtain neurophysiological information from the human brain in a non-invasive way [2], its use is sometimes excessively restricted to the diagnosis of epilepsy, even in patients in whom the level of consciousness should be carefully evaluated [3]. Nevertheless, it should be always remembered that the primary function of the cerebral cortex is to exchange information by generating bioelectrical signals, not only in epilepsy.

In addition to this excessive restriction to epilepsy, EEG is sometimes reported as a subjective method, depending strongly on the interpreter [4–8]. There has been an attempt to reduce inter-rater variability among interpreters by the introduction of a consensus for EEG interpretation [9–13]. Although these consensus and

classifications introduce some objectivity in EEG analysis, the variables are mostly qualitative or binary (present/absent), and specificity is therefore not very high.

In the past few decades, clinicians, neuroscientists, mathematicians, physicists, and engineers (among other experts) have sought a way to overcome these flaws to increase the true field of EEG application and reduce subjectivity in diagnosis. Some research has been devoted to combining EEGs and imaging techniques, mainly magnetic resonance imaging [14–16]. Another direction has been to develop mathematical tools to increase the reliability and deepen the information extracted from neurophysiological recordings. Collectively, this approach is called quantitative EEG (qEEG [17]). A canonical formulation toolbox is not needed to define qEEG. Instead, we can say that every EEG recording that uses any kind of post hoc numerical method to obtain a result about frequency spectrum, synchronization, network dynamics, or anything else of bioelectrical magnitude can be considered qEEG. This approach has been increasing in popularity since the introduction of digitalization in electroencephalography. As an example, in the past few decades, the number of papers referenced in PubMed with the word "qEEG" in the title/abstract rose from two in 1979, to 31 in 1999, and 76 in 2019 (a factor of x38!). However, the use of qEEG in clinical practice is far from being generalized, with the exception of ICUs where long-term monitoring (continuous EEG, cEEG) and qEEG are slowly increasing [18–25].

The time required for a cEEG review is one of the most commonly given reasons for the use of qEEG in the ICU and other diagnostic fields. However, we have taken a different approach to qEEG during cEEG or standard EEG for ambulatory/hospitalized patients: instead of just simplifying seizure detection (another manifestation of the excessive focus on epilepsy), our aim is to obtain a comprehensive and efficient view of the bioelectrical brain physiology/physiopathology in the most objective way. To do this, we have developed qEEG using classical mathematical methods, but in a neurophysiologically and clinically oriented fashion [26].

In this chapter, we want to describe in detail the physiological basis of qEEGs, the method implemented for its quantification, and provide some examples of its use.

2. Physiological basis of qEEG

We have adopted the assumption that EEG is founded in a homeostatic system to obtain the main variables of our method [26–28]. This aspect is of extraordinary relevance because its specific application in different pathologies will lead to specific changes in the different numerical variables obtained. EEG consists of the multivariate spatio-temporal determination of the electrical potentials generated by the brain and recorded on the surface of the scalp. The oscillatory activity of the EEG, in clinical practice, is divided into four bands, depending on its oscillation frequency: delta (δ; 0–4 Hz), theta (θ; 4–8 Hz), alpha (α; 8–13 Hz), and beta (β; 13–30 Hz). Frequencies above 30 Hz, although very important in cognitive research, are not customarily used in clinical practice.

Briefly, the regulation of different bands is given by the following systems [29]:

- Delta. The hyperpolarization of the thalamic-cortical (TC) interstitial pacemaker cells by the nucleus reticularis, together with a lower excitatory effect of the ascending activating reticular system (AARS), releases the spontaneous activity of cortical cells, oscillating at <4 Hz. This oscillation throughout the putamen/globus pallidus inhibits the brainstem nuclei responsible for AARS.

- Theta. There are two theta-generating systems: i) activation of the nucleus reticularis (activated by the AARS) and inhibiting TC neurons and ii) through the mesolimbic system, which includes multiple afferents from the entorhinal cortex, hippocampus, amygdala, septum and anterior cingulate cortex; activating the intralaminar thalamic nuclei, and projecting to layer I of the cerebral cortex.

- Alpha. TC neurons spontaneously oscillate at 6–12 Hz and regulate the excitation of large cortical areas through thalamic-cortico-thalamic re-entry loops. The membrane potential of these cells determines the frequency of oscillation and is regulated by synaptic inputs from the AARS (which includes the intralaminar nuclei of the thalamus), mainly from the brainstem and cortical inputs. Within the cortex, this activity is propagated from some nodes of special importance through interneuronal connections.

- Beta. Originates primarily from cortico-cortical interactions and is facilitated by diffuse activation of the AARS and depolarization of TC cells, allowing the free transfer of information from the sensory systems through the thalamus to the cerebral cortex.

This complex neuroanatomical homeostatic system is probably genetically determined and regulates basal levels of local synchronization, global interactions between different regions, spectral composition, and periodic signal space sampling [30–33].

One of the main limits in our approach is to maintain a close relationship between numerical magnitude variation and the underlying anatomo-functional system. For example, an increase in cortical activity (e.g., a seizure) must always be associated with an increase in β and probably α bands. Obviously, it does not preclude an increase in slower bands, but rising activity in faster bands is mandatory [26].

3. Quantified EEG

There are two branches of analysis: power spectra and synchronization. For both of them, dynamic (i.e., varying along the time) and mean measurements (i.e., mean spectra or mean graph of synchronization) are obtained. The process is summarized in **Figure 1**.

The process used for qEEG followed these steps:

Different length raw records are exported from the EEG device (EEG32, NeuroWorks, XLTEK®, Oakville, ON, Canada) to an ASCII file. Usually, artifacts are excluded by the export of several artifact-free chunks, which are later combined for analysis. We have shown that this process does not changes the main properties analyzed (see below). This process (exportation to an ASCII file) would probably be different for other EEG suppliers, but we have not assessed this possibility. We have computed the export time (t_{export}) as a function of the ASCII file size (S) and obtained a linear expression by means of least-square fitting (r = 0.9947):

$$t_{export}(s) = 0.43S(MB) + 4.13 \quad (1)$$

Although the raw recordings were digitized at 512 or 1024 Hz, we down-sampled to 128 or 256 Hz.

Exported files are digitally are filtered by a sixth-order Butterworth digital filter between 0.5 and 30 Hz.

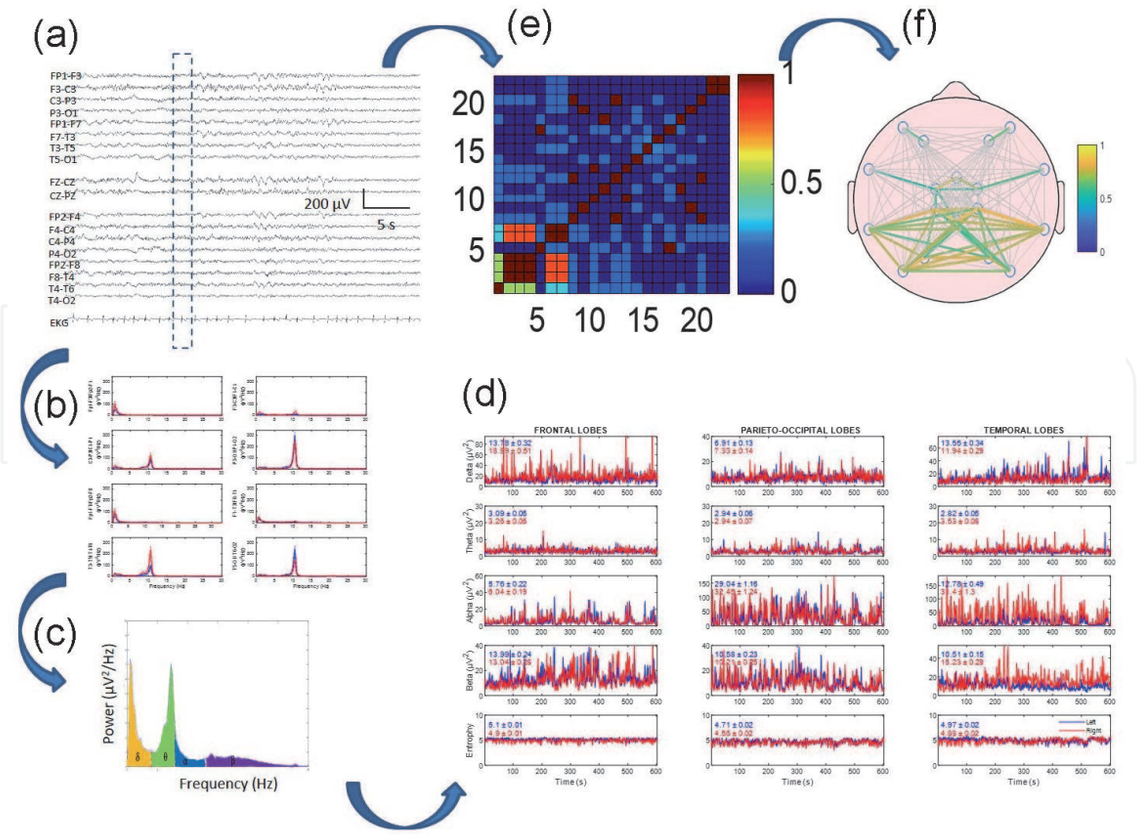

Figure 1.
Method of electroencephalogram (EEG) quantification in two branches: Power spectra (b–d) and synchronization (e,f). (a) Raw EEG tracing. The discontinuous rectangle shows the moving window used for analysis; (b) power spectra for each channel; (c) areas for delta, theta, alpha, and beta bands under the spectrum are highlighted in different colors; (d) dynamics of the four bands (and entropy in the lower row) for every lobe. Mean and SEM values for each tracing are displayed inside each graph. Red and blue lines indicate right and left hemispheres, respectively; (e) correlation matrix for the window; (f) mean correlation computed for all recordings [34].

A differential EEG montage is then reconstructed. Topographic placement of channels is defined on the scalp as the midpoint between the electrode pairs defining the channel; e.g., the Fp1–F3 channel would be placed at the midpoint of the geodesic between the Fp1 and F3 electrodes.

All recording can be divided into different lengths of moving windows (1–5 s each) with different overlaps (between 0 to 50%, but usually 10%). The total length used during the fast Fourier transform (FFT) is directly related to frequency precision in the power spectrum (PS). Overlap is used to minimize the border effect produced by windowing [35].

For each window (n) and frequency (k), we computed the fast Fourier transform (FFT) of the voltage ($V^m(n)$) obtained from each channel (m) to obtain the power spectrum ($S^m_{n,k}$, in $\mu V^2/Hz$). We used the expression:

$$S^m_{n,k} = \sum_{n=0}^{N-1} V^m(n) e^{-i\frac{2\pi}{N}kn}; m = Fp_1, F_3, \ldots \quad (2)$$

We also computed Shannon's spectral entropy (SSE) according to:

$$SSe^m_k = -\sum_{k=0}^{F} p_k \log_2 p_k \quad (3)$$

where F is the maximum frequency computed and p_k is the probability density of S, obtained from the expression:

$$p_k = \frac{S_{n,k}^m}{\sum_{k=0}^{F} S_{n,k}^m \Delta k} \tag{4}$$

We computed the area under the $S_{n,k}^m$ according to the classical segmentation of EEG bands. We used the expression:

$$A_j(k) = \sum_{k=inf}^{sup} S_n^m(k)\Delta k; j = \delta, \theta, \alpha, \beta \tag{5}$$

The expression *sup* refers to the upper limit of each EEG band.

The absolute value of Pearson's correlation coefficient (ρ) is computed for each pair of channels (i,j) according to the expression:

$$\rho_{ij}^k = \frac{\sum_{k=1}^{N_{window}} (x_i(k) - \overline{x}_i) \sum_{k=1}^{N_{window}} \left(x_j(k) - \overline{x}_j\right)}{\sqrt{\sum_{k=1}^{N_{window}} (x_i(k) - \overline{x}_i)^2 \sum_{k=1}^{N_{window}} \left(x_j(k) - \overline{x}_j\right)^2}} \tag{6}$$

where N_{window} is the number of points included in a window (usually 128) and $\overline{x}_i, \overline{x}_j$ represents the mean of both channels.

The mean value of all windows is then computed, obtaining the mean correlation matrix.

Areas of the same band are grouped by cerebral lobes. In the case of the left hemisphere (shown as an example), we grouped the frontal $F = \left\{\frac{\left(Fp_1-F_3\right)+(F_3-C_3)+\left(Fp_1-F_7\right)}{3}\right\}$, parieto-occipital $PO = \left\{\frac{(C_3-P_3)+(P_3-O_1)+(T_5-O_1)}{3}\right\}$, and temporal $T = \left\{\frac{\left(Fp_1-F_7\right)+(F_7-T_3)+(T_3-T_5)+(T_5-O_1)}{4}\right\}$. Channels from the right hemisphere were grouped accordingly. These areas, for both bands (j) and lobes (r), $A_j^r(t); r = F, PO, T$, are plotted as time functions and compared between the hemispheres. The same groups were used to compute *SSe*.

The total time of analysis ($t_{analysis}$) is obtained from this linear expression, which was obtained from least-square fitting:

$$t_{analysis}(s) = 0.32S(MB) + 46.3 \tag{7}$$

From expressions 1 and 7, for a typical 88 MB file (10 min record), we can estimate the time spent in export + analysis as less than 2 min.

We can optionally introduce two time-markers to define different states (e.g., pre-ictal, ictal, and post-ictal periods) in order to statistically compare the changes.

We can optionally export the numerical results to an Excel® file (e.g., mean ± SEM of power, synchronization; and SSe for channels, lobes, and hemispheres). This last step is the most time-consuming (up to 3 min for a custom-length file).

Numerical analysis of EEG recordings was performed with custom-made MATLAB® software (MathWorks, Natick, MA, USA).

For power spectra as well as for synchronization, we can represent measurements either as dynamic time-dependent variables (**Figure 1d**), or as the mean values, averaged over the file (**Figure 1b,f**). Therefore, although complementary, information obtained from both kinds of computations must be interpreted differently. In other words, average measurements are only useful if the stationarity of the record is evident (e.g., basal recordings, well-defined phases of sleep, etc.).

4. Robustness of the method

A very important aspect of any numerical method is its robustness, e.g., the evaluation of the method wherein the results obtained are found to be reliable, even when performed under slightly varied conditions. It is the ability of a method to remain unaffected when slight variations are applied. It is extremely important to check trials of the numerical method within the same group of EEG records under the different conditions of i) down sampling, ii) windowing, or iii) overlapping. Moreover, it is important to check whether synchronization measures are affected by the global analysis of different, non-consecutive chunks.

For this purpose, we selected EEG recordings of five minutes in length, from six control individuals (without any neurological or psychiatric pathology, between 20 and 30 years old, and with no pharmacological treatment). We analyzed each EEG under different conditions, namely:

- Down-sampling at 128 and 512 Hz, (f is for frequency).
- Windows of 1, 3 or 5 s (w).
- Overlapping at 10, 20, or 40% (o).

Overall, we had 18 combinations for frequency/windows/overlapping (f,w,o).

The structure of EEG for each patient (p_i, i = 1,2, ... 6) can be described by a 10-element vector as:

$$p_i = \left(\delta_i^l, \theta_i^l, \alpha_i^l, \beta_i^l, \rho_i^l, \delta_i^r, \theta_i^r, \alpha_i^r, \beta_i^r, \rho_i^r\right); l = left, r = right \quad (8)$$

Obviously, every structure can be described as $p_i(f, w, o)$. A robust method should not affect the structure of EEG for the same patient, irrespective of changes in absolute values. For each patient, we have plotted along the x-axis (coordinates of EEG structure) the normalized band values and correlations for all of the 18 combinations (**Figure 2**).

From **Figure 2**, we can observe that different combinations cannot affect the structure of EEG.

The effect of multiple compositions of the analyzed file on synchronicity was assessed as follows: an EEG record of 3 min was analyzed. Then, the same record was exported in three different chunks, and a new analysis was performed on a recombined file with the parts randomly ordered (1,3,2/2,1,3/2,3,1/3,1,2 or 3,2,1). We did not observed any difference in synchronization between the whole record and a recombined one (not shown).

In summary, these results demonstrate that the method is highly robust, at least for the limits addressed.

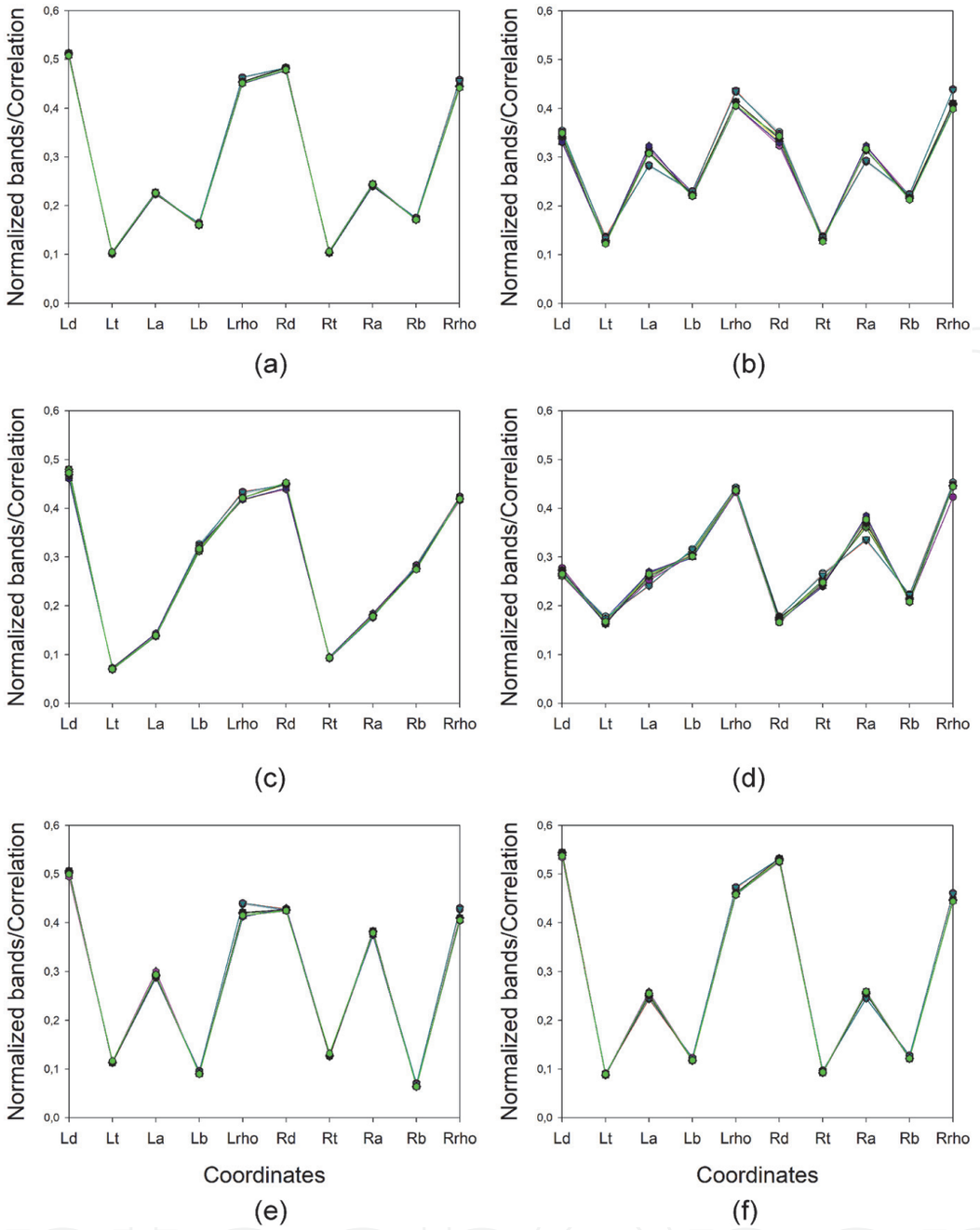

Figure 2.
Structures of EEG for the 18 combinations of variables for (a) patient #1, (b) patient #2, (c) patient #3, (d) patient #4, (e) patient #5 and (f) patient #6. L = left, R = right, d = delta, t = theta, a = alpha, b = beta, and rho = correlation.

5. Some examples of the utility of qEEG

It is out of the scope of this chapter to illustrate the objective and quantified difference between the classical, *de visu*, analysis of EEG and qEEG. Instead, we will provide some examples of qEEG application to real clinical problems and the results. In these examples it will be shown that information obtained by qEEG clearly exceeds the possibility of *de visu* analysis.

5.1 Differentiation between periodic patterns and seizures

Patients in the ICU usually undergo a limited clinical neurological examination because of either structurally or functionally altered conditions of the central

nervous system (CNS) or due to the effects of drugs used for sedoanalgesia [36]. Therefore, we can evaluate brain function in these conditions by EEG. However, a dynamic evolution of injury is frequently observed in critically ill patients due to the occurrence of epileptic seizures (ES), status epilepticus (SE), or other brain insults [37, 38]. In this sense, cEEG allows the functional assessment of the cerebral cortex in real time for prolonged periods. It has been proven to be an extraordinarily useful tool for detecting electrographic seizures and non-convulsive epileptic status (NCES), modifying treatment and assessing the functional prognosis [10, 11, 39–42].

The particularity of cEEG records of patients in the ICU comprises a high frequency of artifacts and frequently observed rhythmic and periodic patterns, which are easily confused with seizures. Both can be difficult to interpret not only in a raw EEG but also with the qEEG tools currently used [43, 44]. As indicated above, the use of multiple drugs acting on the CNS and primary and secondary injuries profoundly affect the bioelectrical brain dynamics. Therefore, it can be quite difficult to differentiate between bursts of periodic activity (BPA) and true ES/SE. The main problem is that EEG patterns analyzed *de visu* do not always exhibit the sharp morphology of ES/SE of not-ICU patients.

According to the ILAE, an ES is a transient occurrence of signs and/or symptoms due to abnormal excessive or synchronous neuronal activity in the cortex of the brain [45]. Signs/symptoms are usually excluded in critically ill patients, but the excessive activity of the cortex is mandatory for a positive identification. We have used this pathophysiological feature for the numerical definition of ES. Therefore, we can use this method to exclude epilepsy in those cases where α/β activity does not change (or even decreases) during the event (see below). The limits of change for the different bands (**Table 1**) can be used to distinguish PBA from ES.

From this table we can observe that the superposition is very high for δ bands (i.e., this band is not discriminative), low for θ and *Se,* and practically null for α and β bands. Therefore, the intervals for increments of normalized activity defining an ES in these types of patients are as follows (excluding superposition and rounding): $\delta_F = [119, 166]$; $\theta_F = [173, 264]$; $\theta_{PO} = [168, 248]$; $\theta_T = [151, 274]$; $\alpha_F = [159, 244]$; $\alpha_{PO} = [159, 244]$; $\alpha_T = [159, 244]$; $\beta_F = [141, 374]$; $\beta_{PO} = [146, 262]$; $\beta_T = [141, 374]$; $Se_F = [97, 110]$; $Se_{PO} = [98, 107]$; $Se_T = [98, 104]$.

We have defined the numerical features of ES and BPA in critically ill patients using the pathophysiological definition of epilepsy. This will facilitate its identification in clinical practice, allowing a precocious and more adequate treatment.

5.2 Specific characterization of encephalopathy in SARS-CoV-2 patients

Neurological complications in COVID-19-infected patients have been reported. The CNS effects reported include encephalitis, toxic encephalopathy, ageusia and anosmia, headaches, or acute cerebrovascular disease [46–52]. The mechanisms of CNS infection in the pathophysiology of COVID-19 are still debated, and it has been proposed to result from direct invasion through the blood–brain barrier, a neuronal pathway, hypoxia damage, immune-response mediated injury, or angiotensin-converter enzyme 2 activity, among other possibilities [47, 53, 54]. Encephalopathy refers clinically to state of impaired cognition, generally acute or subacute [55]. Descriptions *de visu* of EEG are based on classical analysis by visual inspection and not on specific features [56–58].

We applied our method of qEEG to patients discharged from the ICU after COVID-19 infection [34]. We used two control groups from patients previously studied in our hospital: (i) patients with infectious toxic encephalopathy (ENC) and (ii) patients after cardiorespiratory arrest (CRA), as an example of severe hypoxic insult to the CNS.

Variable	State	Frontal	Sup (%)	Parieto-occipital	Sup (%)	Temporal	Sup (%)
Delta	ES	111.8–234.0	55.4	123.8–276.8	91.3	118.4–247.6	86.1
	BPA	166.3–370.4		137.1–278.7		136.3–253.9	
Theta	ES	158.2–264.0	14.2	166.7–247.7	1.6	139.2–230.5	19.9
	BPA	92.8–173.2		84.3–168.0		93.1–157.4	
Alpha	ES	158.8–244.0	0	146.0–248.6	0	144.3–243.5	0
	BPA	75.0–137.8		79.7–134.1		82.7–135.6	
Beta	ES	141.9–373.6	0	146.7–261.8	0	136.5–274.4	10.4
	BPA	77.1–137.8		82.2–137-2		95.1–150.8	
Entropy	ES	95.5–109.5	10.7	96.2–106.7	12.4	96.1–104.8	19.5
	BPA	78.9–97.0		84.3–97.5		82.3–97.8	

Table 1.
Inter-percentile 25–75 intervals for bands and lobes in BPA and ES. Superposition is indicated with respect to the ES interval [26].

Visually, in COVID-19, EEG records the apparent absence of delta/theta activity conferred a near-physiological aspect to the recordings. Despite the different visual aspects appearing between ENC and COVID-19, the mean spectra by channel were quite similar. Examples of typical recordings are shown in **Figure 3**.

We assessed the specific differences for each band in ENC, COVID-19, and CRA patients. Subsequently, we performed one-way ANOVA (ANOVA on ranks when normality failed) for each lobe and band, and for SSe and synchronization (**Figure 4**).

The pattern of ENC and CRA was clearly different for all bands. However, the COVID-19 group was not completely different from the ENC and CRA groups, although it was evidently observed that the distribution is between the two extreme groups. Nonetheless, the behavior of temporal lobes clearly differs for the ENC and COVID-19 groups for the δ, α, and β bands. Contrary to EEG bands, SSe was higher for the COVID-19 group and lower for the ENC group. In fact, SSe was different for all groups at all lobes. This result may be surprising considering the kind of spectra shown in **Figure 3c**, where the distribution was apparently more complex. However, the presence of α and β bands (scarcely present in the CRA group) increased the SSe for COVID-19 patients.

Finally, although ρ was not as different between groups as SSe, a clear difference was seen in the hemispheric synchronization and frontal lobes of ENC and COVID-19 patients, with lower synchronization for the latter group.

In summary, we have demonstrated that qEEG can differentiate between encephalopathy types, and we have described the numerical features of each. In this context, we show that COVID-19 patients display EEG structures that are truly distinguishable from those of both infectious toxic encephalopathy and encephalopathies of patients who experience severe hypoxic conditions. Significantly, the EEG pattern of COVID-19 patients was between those of the ENC and CRA groups. Therefore, it can be speculated that hypoxia may show some participation in this electroclinical entity. However, the EEG structures of the CRA and COVID-19 groups were different enough to consider that other factors besides hypoxia must be responsible for the bioelectrical pattern.

It is extremely relevant to bear in mind that COVID-19 patients showed mild to severe cognitive symptoms despite *de visu* quasi-normal recordings. However, the severe numerical alterations of temporal lobes spectra, structure of SSe and

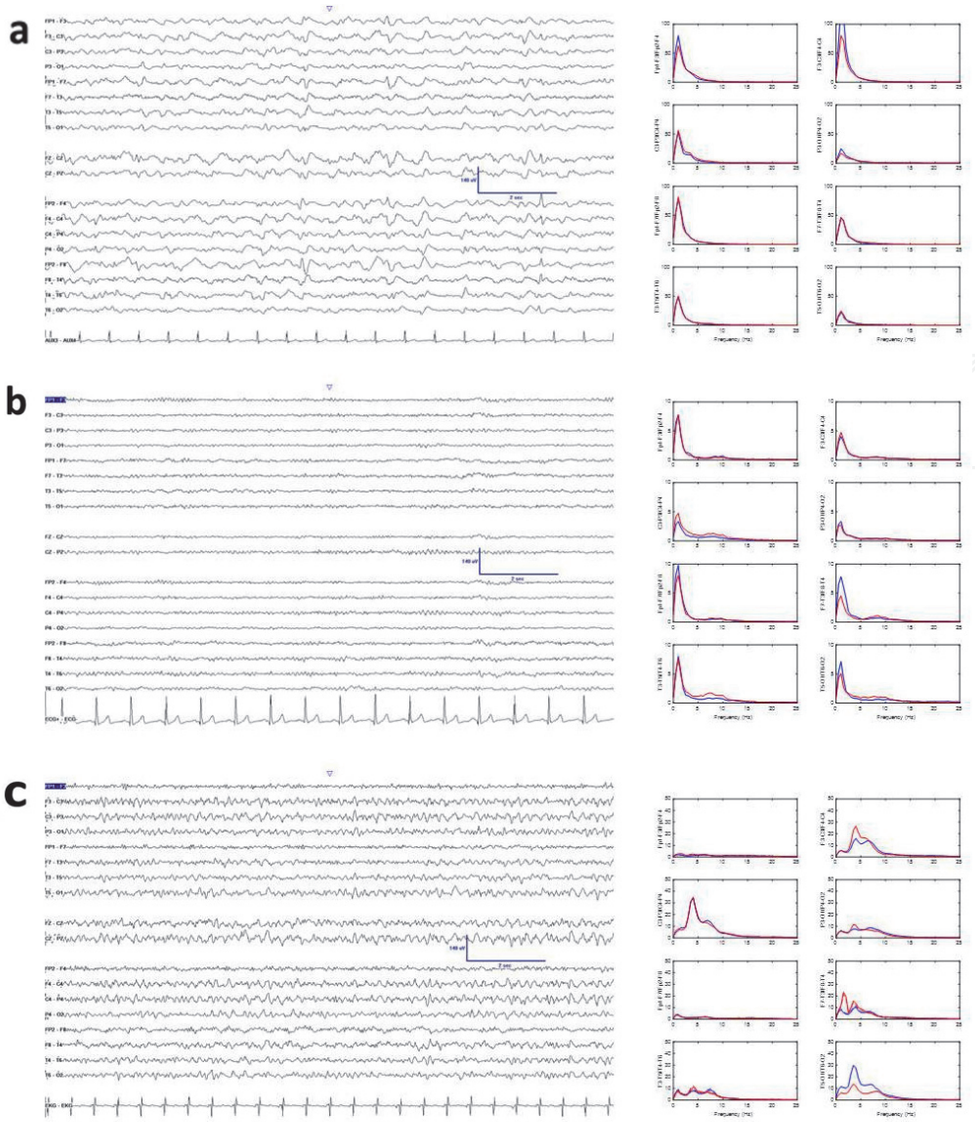

Figure 3.
Examples of raw recordings: (a) encephalopathy (ENC), (b) COVID-19, and (c) cardiorespiratory arrest (CRA). Right column shows mean spectra for channels. Red and blue lines indicate right and left hemispheres, respectively. Y-axis units in μV²/Hz [34].

synchronization were highly different and are probably explained by symptomatology with quasi-normal EEG traces.

5.3 Continuous EEG monitoring in ICU

Long-term EEG monitoring in the ICU (cEEG) has been one of the main developing fields of electroencephalography in recent years. There are several methods used for EEG monitoring, and most of them share a similar philosophy: to identify the presence of seizure/status epilepticus to make the information of monitoring easy and fast. As stated above, we think that this reductionist approach impoverishes the scope of electroencephalography.

We systematically used qEEG during cEEG for the below indications:

- Monitoring the presence of ES/SE. More useful than identifying the presence of ES, qEEG is essential to discriminate between epileptic and non-epileptic patters, as we stated above.

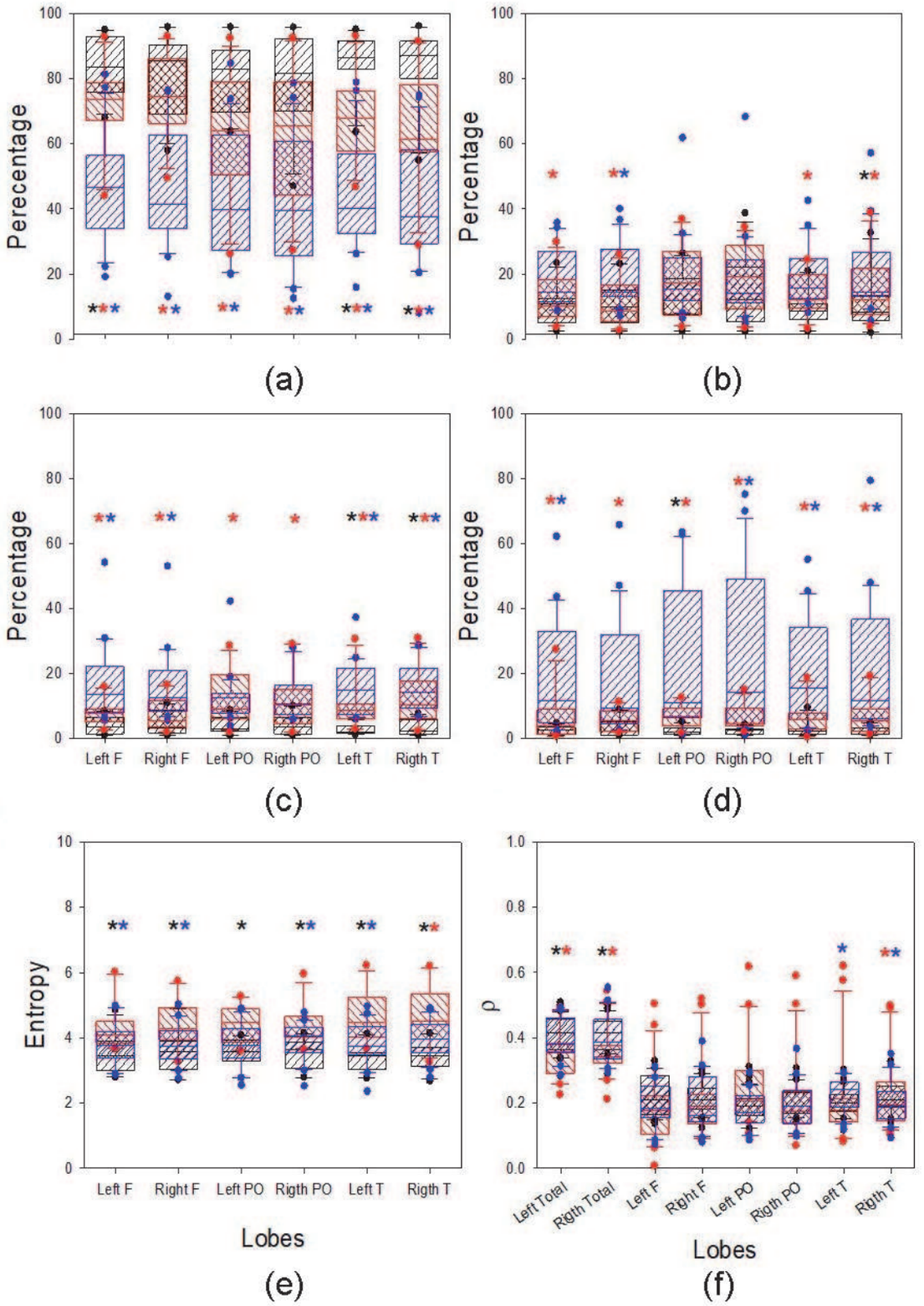

Figure 4.
Box plots showing the comparison of EEG structures for different bands: (a) delta, (b) theta, (c) alpha, and (d) beta, (e) Se; (f) ρ. striped black box: ECN; striped red box: COVID-19; striped blue box: CRA; black asterisk: Difference between ENC and COVID-19; red asterisk: Difference between ENC and CRA; blue asterisk: Difference between COVID-19 and CRA.

- Titration of sedation/anti-epileptic drugs (AEDs). Identifying changes in background from the variations in spectra or mean values of specific EEG bands is mandatory to increase/decrease the dose of sedation. Additionally, AEDs are adjusted with the help of qEEG, although *de visu* inspection of irritative activity is mandatory.

- Long-term recordings in patients with alterations of consciousness without sedo-analgesia to evaluate brain physiology. Severe encephalopathy can induce a low-consciousness level. These recordings typically lack irritative activity, and changes in the background are slow. However, these changes correlate with the level of consciousness and predict the outcome. Therefore, it is important identify changes to adjust treatment as soon as possible, especially to avoid unnecessary therapeutic actions.

In this way, we have performed more than 250 cEEG + qEEG in the ICU in the last five years. This is a time-consuming task (especially considering that every cEEG takes 1.4–4.3 days (inter-percentile 25–75 range)), but the clinical utiliy is clear because the demand increased from 1.0 ± 0.2 cEEG/month in 2015 to 5.5 ± 0.8 cEEG/month in 2019.

5.4 Utility in dementia

There are numerous articles in the literature showing that the initial phases of dementia can be detected by qEEG [59–63]. We have used our numerical method in patients with either minimum cognitive impairment (MCI) or aphasia. Obviously, the *de visu* analysis of raw recordings shows only a nearly normal aspect or low-voltage. However, numerical analysis can show very relevant facts that are not observable by eye (**Figure 5**).

At this time, we are conducting a study to identify specific properties of different pathologies (sub-types of primary aphasia, Alzheimer disease, vascular dementia, etc). Although we have not yet defined different groups of features specific to each pathology, what is clear from the above figure is that connectivity is a magnitude that is affected early and consistently in most cognitive alterations.

5.5 Other examples of qEEG utility

Finally, we provide two more representative examples of diagnosis highly aided by the use of qEEG.

Case 1. A 17-year-old male patient with severe cognitive and behavioral impairment, secondary to severe epileptic encephalopathy due to refractory epilepsy in childhood after a central nervous system infection. Daily seizure frequency, with countless seizures per day. In treatment with zonisamide (400 mg), valproic acid (1200 mg), oxcarbazepine (1400 mg), and clobazam (10 mg) daily. Rectal diazepam 10 mg if required. A video of EEG is performed in which it is observed that during sleep, the patient exhibits several episodes of lateral head movement and growls. *De visu* recordings (**Figure 6a**) can be described as global desynchronization. However, the dynamics of the EEG bands show a decrease (practically total) for all the bands (**Figure 6b**). As stated above, epilepsy is expected to be accompanied by an increase in cortical activity (α and β bands). Therefore, this event cannot be identified as epileptic.

Although the patient also presented true epileptic events, the number of these was substantially lowered and AED was adjusted according to the real number of ES. The final diagnosis for this event was a nonepileptic behavioral disorder, secondary to severe epileptic encephalopathy.

Case 2. A 22-year-old female diagnosed with epilepsy at the age of 14 years and with anxious-depressive illness from the age of 20 years. The applied treatment was lamotrigine (100 mg/day) and clonazepam (0.5 mg/8 h). Seizures occurred every 2–3 days, described as the perception of black dots in the visual field, weakness, loss of consciousness and muscle tone, loss of balance and falling to the ground. During

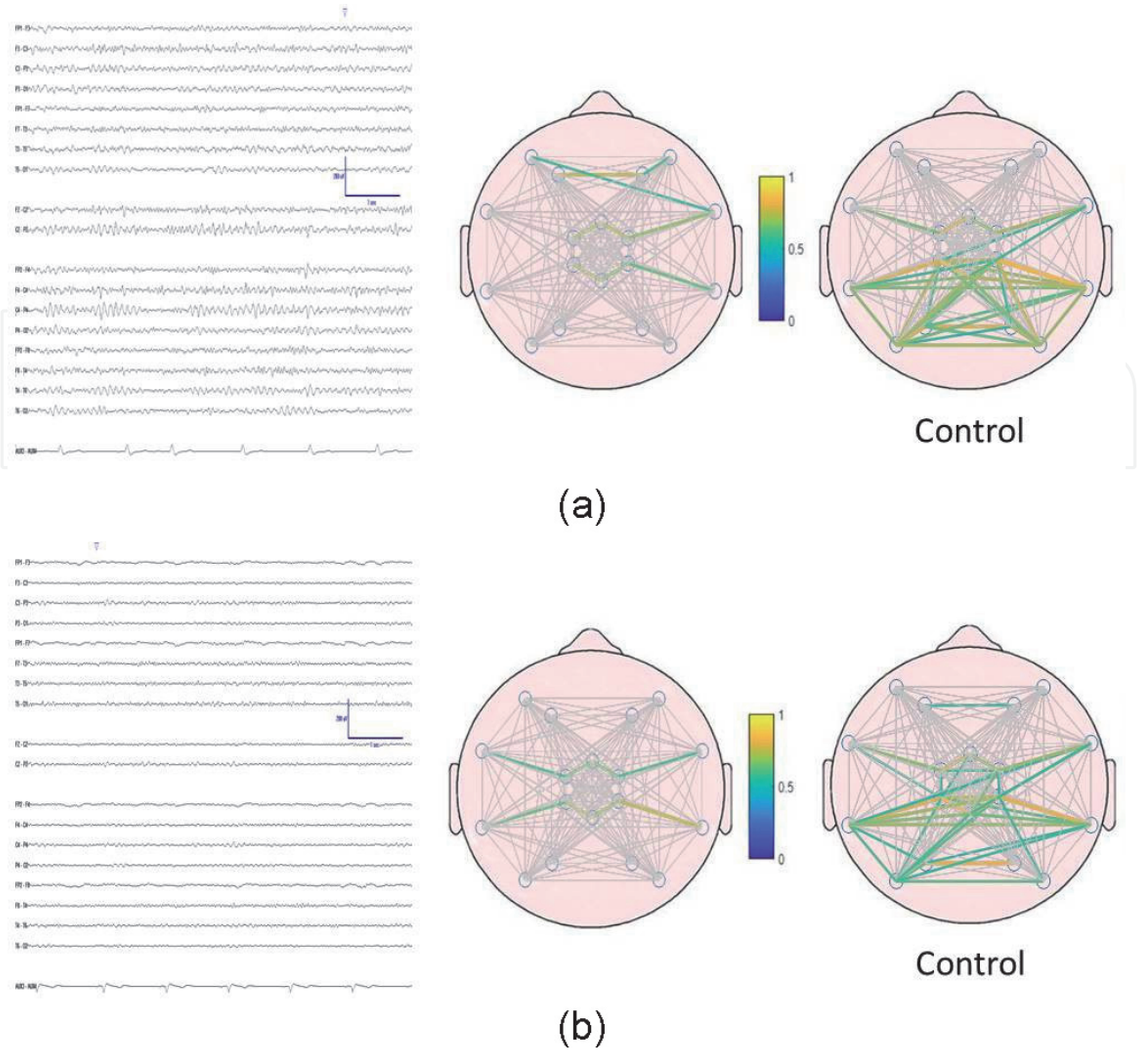

Figure 5.
Initial steps of dementia. (a) Example of a male with primary aphasia and (b) a female with MCI. Left column = raw recordings of both patients; middle column = connectogram for patients; right column = connectogram of a control volunteer of the same sex and age (± 5 years).

telemetry, we recorded one episode of black dot perception followed by a loss of consciousness while in bed. *De visu* EEG recordings showed no significant changes (**Figure 7a**). However, the dynamic variation of EEG bands indicated a generalized decrease, except for the occipital α band, which increased after the eyes closed (**Figure 7b**).

The final diagnosis was psychogenic non-epileptic seizure (PNES), and the AEDs were slowly removed.

6. Discussion

Numerous methods have been used for qEEG, although they are rarely used in daily clinical practice. There is, therefore, a huge gap between the promising (even spectacular) results obtained with qEEG and its practical usefulness. To the best of the knowledge of the authors, this issue has not been systematically addressed, although it has been said that electroencephalographers have poor trust in mathematical models [2, 17].

The degree of mathematical complexity and abstraction is quite different among the methods proposed. Not all of the mathematical models can be included in the same category, and it is of extreme importance that mathematical solutions be

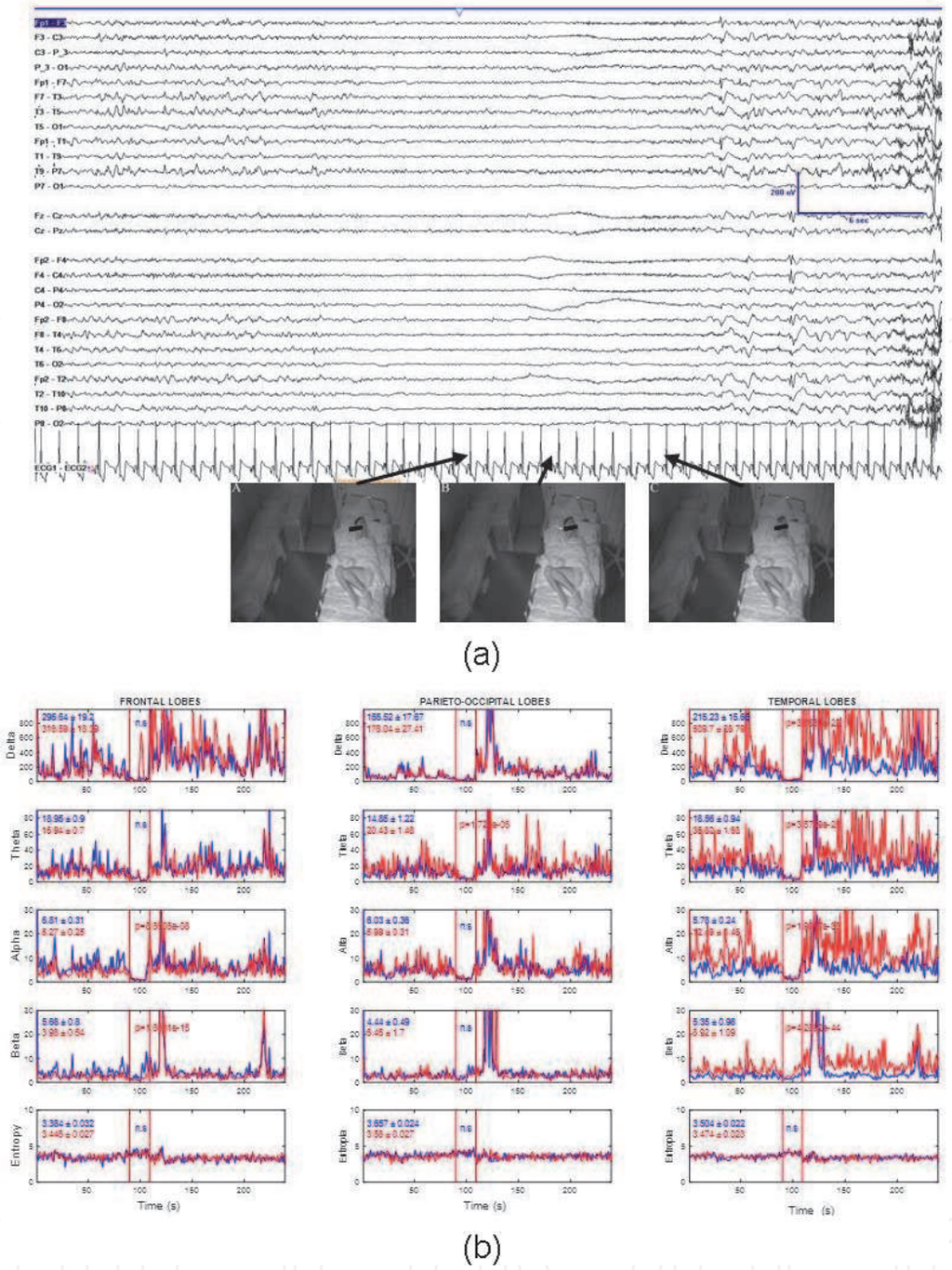

Figure 6.
Box plots showing a comparison of EEG structure for different bands: (a) raw recording during a complete event during sleep. The images under the recordings correspond to the periods indicated by arrows. (b) Lobar dynamics of EEG bands during the entire event (vertical red lines). Blue = left hemisphere; red = right hemisphere.

robust with respect to physiological assumptions [2]. Then, some procedures require relatively simple and involve straightforward methods as FFT [26, 34, 64–66] and synchronicity measurements [67, 68], approaches that clinicians are familiar with. In contrast, other numerical methods are more complex, or the mathematical approach deviates from physiological assumptions [69–74], and this probably takes neurophysiologists out of their comfort zone.

We have developed a robust method that is physiologically founded and easy to use in daily clinical practice. The tools selected are neither unique nor are they necessarily the best. Other tools (e.g., coherence) can be implemented. A careful comparison between these methods will decide the fitted procedure for each

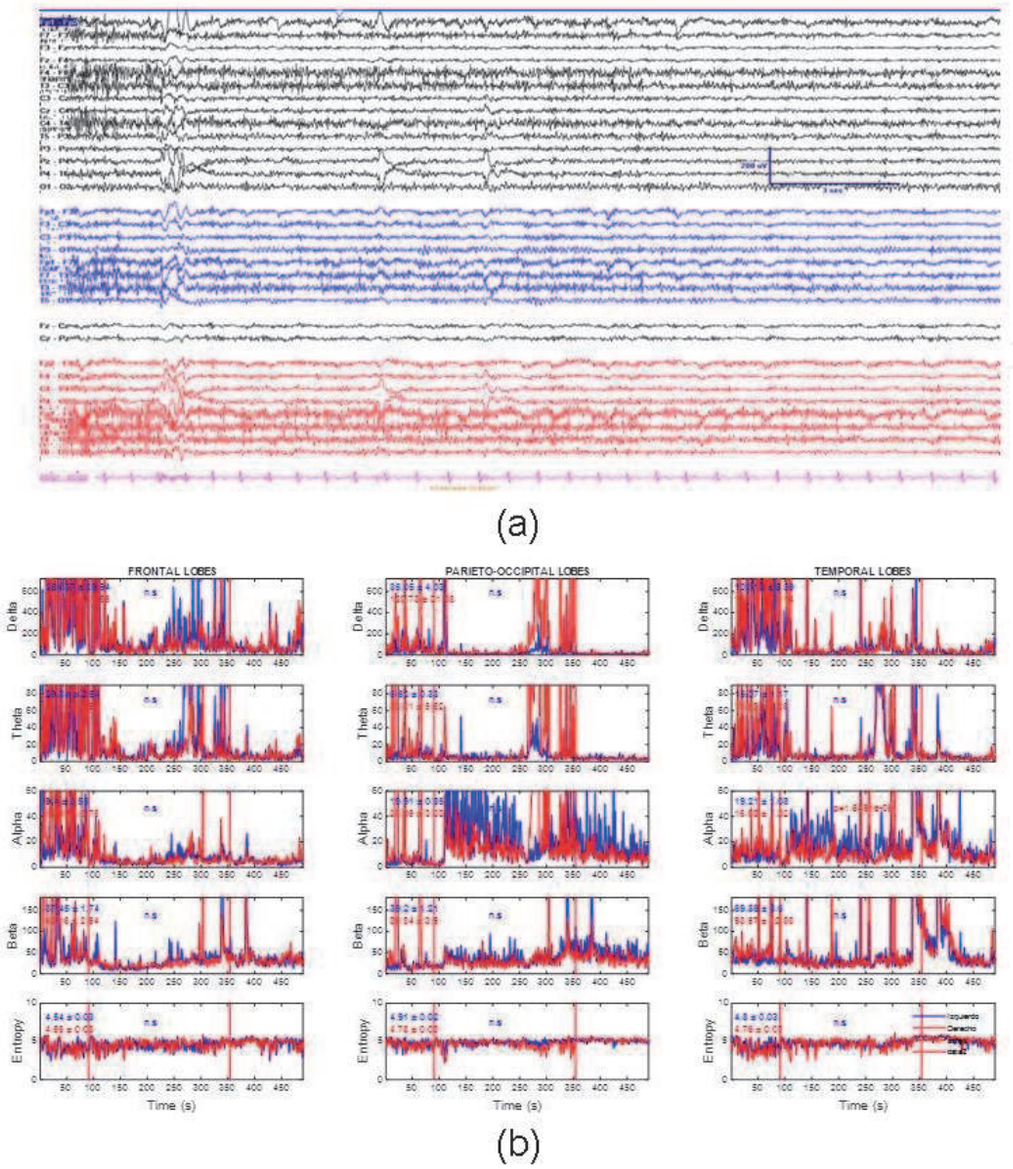

Figure 7.
Psychogenic non epileptic seizure (a) raw recordings (in transverse and double banana differential montages) during the event. (b) Lobar dynamics of EEG bands during the entire event (vertical red lines). Blue = left hemisphere; red = right hemisphere.

pathology. From the beginning of 2016, we have performed more than 4100 analyses and used this toolbox in most patients, even those with EEG apparently evident. We did not use qEEG only when the record included so many artifacts (e.g., in agitated patients) that the results would not be reliable.

The method described can be implemented to automatically differentiate between paroxysmal events and ES during the long-term monitoring of ICU patients. This feature is very relevant for clinicians because it can shorten the review time, particularly during long cEEG, and can help apply adequate therapeutic measures, avoiding pharmacological blind trials that only delay correct treatment, increasing the inefficacy of treatment and diminishing the probability of recuperation. Therefore, considering that "time is brain", a fast and accurate treatment is mandatory to increase the probability of a good outcome.

Finally, it is extremely important to keep in mind that qEEG is only a tool to help better understand and diagnose brain pathophysiology; therefore, it should not be thought that numerical analysis (at least as we use it today) is enough, without evaluation by an expert, to make an automatic diagnosis. Not all brain pathologies

are likely to benefit to the same degree from analysis. For example, the method described in this chapter is not well fitted to detect low-frequency transitory waves as medium/small focal epileptiform discharges, although visual inspection can identify them very well. However, patterns that are not readily visible in *de visu* analysis (e.g., asymmetries in power spectra compositions) are easily detected.

7. Conclusions

We can summarize the conclusions of this work as follows:

- qEEG is a robust and non-time-consuming method that is able to produce numerical and objective values of several bioelectrical magnitudes with clinical significance.

- qEEG increases and facilitates diagnoses that are otherwise exceedingly difficult to obtain by *de visu* inspection. Therefore, the scope of the true applicability of EEG is expanded far beyond epilepsy.

- We propose that qEEG use should be expanded globally for daily clinical practice. Thus, clinical neurophysiologists should be informed of the methods of numerical analysis procedures.

Acknowledgements

This work was financed by a grant from the Ministerio de Sanidad FIS PI17/02193, ISCIII (Instituto de Salud Carlos III) and partially supported by FEDER (Fonds Europeen de Developpement Economique et Regional).

Conflict of interest

The authors declare no conflict of interest.

Author details

Jesús Pastor*, Lorena Vega-Zelaya and Elena Martín Abad
Clinical Neurophysiology, Hospital Universitario La Princesa, Madrid, Spain

*Address all correspondence to: jesus.pastor@salud.madrid.org

References

[1] Berger H: Uber das elektroenzephalogramm des Menschen. Arch. Psychiatr. Nervenk. 1929; 87: 527–570.

[2] Nunez PL, Srinivasan , editors. Electric fields of the brain. The neurophysics of EEG. 2nd ed. Oxford University Press; 2006.

[3] Pellinen J, Carroll E, Friedman D, Boffa M, Dugan P, Friedman DE, Gazzola D, Jongeling A, Rodriguez aj, Holmes M: Continous EEG findings in patients with COVID-19 infection admitted to a New York academic hospital system. Epilepsia; 2020; 00: 1–9; doi.org/10.1111/epi.16667

[4] Wendt SL, Welinder P, Sorensen HB, Peppard PE, Jennum P, Perona P, Mignot E, Warby SC: Inter-expert and intra-expert reliability in sleep spindle scoring. Clin Neurophysiol. 2015;126(8): 1548–56. doi: 10.1016/j.clinph.2014.10.158.

[5] Halford JJ, Shiau D, Desrochers JA, Kolls BJ, Dean BC, Waters CG, Azar NJ, Haas KF, Kutluay E, Martz GU, Sinha SR, Kern RT, Kelly KM, Sackellares JC, LaRoche SM: Inter-rater agreement on identification of electrographic seizures and periodic discharges in ICU EEG recordings. Clin Neurophysiol. 2015; 126(9):1661–9. doi: 10.1016/j.clinph.2014.11.008.

[6] Halford JJ, Arain A, Kalamangalam GP, LaRoche SM, Leonardo B, Basha M, Azar NJ, Kutluay E, Martz GU, Bethany WJ, Waters CG, Dean BC: Characteristics of EEG Interpreters Associated With Higher Interrater Agreement. J Clin Neurophysiol. 2017 Mar;34(2):168–173. doi: 10.1097/WNP.0000000000000344.

[7] Halford JJ, Westover MB, LaRoche SM, Macken MP, Kutluay E, Edwards JC, Bonilha L, Kalamangalam GP, Ding K, Hopp JL, Arain A, Dawson RA, Martz GU, Wolf BJ, Waters CG, Dean BC: Interictal Epileptiform Discharge Detection in EEG in Different Practice Settings. J Clin Neurophysiol. 2018 Sep;35(5):375–380. doi: 10.1097/WNP.0000000000000492.

[8] Jing J, Herlopian A, Karakis I, Ng M, Halford JJ, Lam A, Maus D, Chan F, Dolatshahi M, Muniz C, Chu C, Sacca V, Pathmanathan J, Ge W, Sun H, Dauwels J, Cole AJ, Hoch DB, Cash SS, Westover MB: Interrater Reliability of Experts in Identifying Interictal Epileptiform Discharges in Electroencephalograms. JAMA Neurol. 2019;77(1):49–57. doi: 10.1001/jamaneurol.2019.3531

[9] Hirsch LJ, LaRoche SM, Gaspard N, Gerard E, Svoronos A, Herman ST, Mani R, Arif H, Jette N, Minazad Y, Kerrigan JF, Vespa P, Hantus S, Claassen J, Young GB, So E, Kaplan PW, Nuwer MR, Fountain NB, Drislane FW: American Clinical Neurophysiology Society's Standardized Critical Care EEG Terminology: 2012 version. J Clin Neurophysiol. 2013 Feb;30(1):1–27. doi: 10.1097/WNP.0b013e3182784729. PMID: 23377439.

[10] Herman ST, Abend NS, Bleck TP, Chapman KE, Drislane FW, Emerson RG, Gerard EE, Hahn CD, Husain AM, Kaplan PW, LaRoche SM, Nuwer MR, Quigg M, Riviello JJ, Schmitt SE, Simmons LA, Tsuchida TN, Hirsch LJ: Critical Care Continuous EEG Task Force of the American Clinical Neurophysiology Society. Consensus statement on continuous EEG in critically ill adults and children, part I: indications. J Clin Neurophysiol. 2015 Apr;32(2):87–95. doi: 10.1097/WNP.0000000000000166.

[11] Herman ST, Abend NS, Bleck TP, Chapman KE, Drislane FW, Emerson RG, Gerard EE, Hahn CD, Husain AM, Kaplan PW, LaRoche SM,

Nuwer MR, Quigg M, Riviello JJ, Schmitt SE, Simmons LA, Tsuchida TN, Hirsch LJ: Critical Care Continuous EEG Task Force of the American Clinical Neurophysiology Society. Consensus statement on continuous EEG in critically ill adults and children, part II: personnel, technical specifications, and clinical practice. J Clin Neurophysiol. 2015 Apr;32(2):96–108. doi: 10.1097/WNP.0000000000000165.

[12] Admiraal MM, van Rootselaar AF, Horn J: International consensus on EEG reactivity testing after cardiac arrest: Towards standardization. Resuscitation. 2018 Oct;131:36–41. doi: 10.1016/j.resuscitation.2018.07.025.

[13] Claassen J, Taccone FS, Horn P, Holtkamp M, Stocchetti N, Oddo M: Neurointensive Care Section of the European Society of Intensive Care Medicine. Recommendations on the use of EEG monitoring in critically ill patients: consensus statement from the neurointensive care section of the ESICM. Intensive Care Med. 2013 Aug;39(8):1337–51. doi: 10.1007/s00134-013-2938-4.

[14] Robertson JA, Thomas AW, Prato FS, Johansson M, Nittby H: Simultaneous fMRI and EEG during the multi-source interference task. PLoS One. 2014 Dec 9;9(12):e114599. doi: 10.1371/journal.pone.0114599

[15] Klein C, Hänggi J, Luechinger R, Jäncke L: MRI with and without a high-density EEG cap—what makes the difference? Neuroimage. 2015;106:189–97. doi: 10.1016/j.neuroimage.2014.11.053.

[16] Omidvarnia A, Kowalczyk MA, Pedersen M, Jackson GD: Towards fast and reliable simultaneous EEG-fMRI analysis of epilepsy with automatic spike detection. Clin Neurophysiol. 2019 Mar;130(3):368–378. doi: 10.1016/j.clinph.2018.11.024.

[17] Vega-Zelaya L, Garnés-Camarena O, Sánz-García A, Ortega GJ, Pastor J: Mathematical foundations of quantified electroencephalography. Clinical Advances in Neurophysiology. Chapter 3. Avid Science. 2016; February, 10.

[18] Hirsch LJ: Continuous EEG monitoring in the intensive care unit: an overview. J Clin Neurophysiol. 2004; 21: 332–340.

[19] Kennedy JD, Gerard EE: Continuous EEG monitoring in the intensive care unit. Curr Neurol Neurosci Rep. 2012; 12: 419–428.

[20] Ney JP, van der Goes DN, Nuwer MR, Nelson L, Eccher MA: Continuous and routine EEG in intensive care: utilization and outcomes, United States 2005–2009. Neurology. 2013; 81: 2002–2008.

[21] Sutter R, Stevens RD, Kaplan PW: Continuous electroencephalographic monitoring in critically ill patients: indications, limitations and strategies. Crit Care Med. 2013; 41: 1124–32.

[22] Sackellares JC, Shiau DS, Halford JJ, LaRoche SM, Kelly KM: Quantitative EEG analysis for automated detection of nonconvulsive seizures in intensive care units. Epilepsy Behav. 2011, 22, S69–S73.

[23] Dericioglu N, Yetim E, Bas DF, Bilgen N, Caglar G, Arsava EM, Topcuoglu MA: Non-expert use of quantitative EEG displays for seizure identification in the adult neuro-intensive care unit. Epilepsy Res. 2015, 109, 48–56.

[24] Haider HA, Esteller R, Hahn CD, Westover MB, Halford JJ, Lee JW, Shafi MM, Gaspard N, Herman ST, Gerard EE, Hirsch LJ, Ehrenberg JA, LaRoche SM: Critical Care EEG Monitoring Research Consortium. Sensitivity of quantitative EEG for seizure identification in the intensive care unit. Neurology. 2016 Aug 30;87 (9):935–44. doi: 10.1212/

WNL.0000000000003034. Epub 2016 Jul 27. PMID: 27466474; PMCID: PMC5035158.

[25] Zubler F, Bandarabadi M, Kurmann R, Steimer A, Gast H, Schindler K: Quantitative EEG in the Intensive Care Unit. Epileptologie. 2016; 33: 166–172

[26] Vega-Zelaya L, Martín Abad E, Pastor J: Quantified EEG for the characterization of epileptic seizures versus periodic activity in critically ill patients. Brain Sci. 2020, 10, 158; doi: 10.3390/brainsci10030158.

[27] John ER, Ahn H, Prichep, LS, Trepetin M, Brown D, Kaye H: Developmental equations for the electroencephalogram. Science 1980, 210, 1255–1258.

[28] John ER, Prichep LS, Easton P: Normative data banks and neurometrics: Basic concepts, methods and results of norm construction. In Handbook of Electroencephalography and Clinical Neurophysiology, Vol. I; Gevins, A.S., Remond, A., Eds.; Elsevier: Amsterdam, The Netherlands, 1987; pp. 449–495.

[29] John ER: The neurophysics of consciousness. Brain Res. Brain Res. Rev. 2002, 39, 1–28.

[30] Szava S, Valdes P, Biscay R, Galan L, Bosch J, Clark I, Jimenez JC: High resolution quantitative EEG analysis. Brain Topogr. 1994, 6, 211–219.

[31] Hughes JR, John ER: Conventional and quantitative electroencephalography in psychiatry. J. Neuropsychiatry Clin. Neurosci. 1999, 11, 190–208.

[32] Kondacs A, Szabo M: Long-term intra-individual variability of the background EEG in normal. Clin. Neurophysiol. 1999, 110, 1708–1716.

[33] Kropotov JD. Quantitative EEG, event-related potentials and neurotherapy. Academic Press, 2009, Amsterdam.

[34] Pastor J, Vega-Zelaya L, Martin Abad E: Specific EEG encephalopathic pattern in SARS-CoV-2 patients. J. Clin. Med, 2020, 9,1545; doi:103390/ jcm9051545.

[35] Van Drongelen, W. Signal Processing for Neuroscientists; Elsevier: Amsterdam, The Netherlands, 2007.

[36] Sutter R, Kaplan PW: Clinical and electroencephalographic correlates of acute encephalopathy. J Clin Neurophysiol. 2013 Oct;30(5):443–53. doi:10.1097/WNP.0b013e3182a73bc2.

[37] Lorente L, Martín MM, González-Rivero AF, Argueso M, Ramos L, Solé-Violán J, Cáceres JJ, Jiménez A, Borreguero-León JM: Serum levels of caspase-cleaved cytokeratin-18 in patients with severe traumatic brain injury are associated with mortality: a pilot study. PLoS One 2015, 10, e0121739

[38] Lorente L, Martín MM, González-Rivero AF, Pérez-Cejas A, Argueso M, Ramos L, Solé-Violán J, Cáceres JJ, Jiménez A, García-Marín V: High Serum Caspase-Cleaved Cytokeratin-18 Levels and Mortality of Traumatic Brain Injury Patients. Brain Sci. 2019 Oct 10;9(10). pii: E269. doi: 10.3390/brainsci9100269

[39] Pandian JD, Cascino GD, So EL, Manno E, Fulgham JR: Digital video-electroencephalographic monitoring in the neurological-neurosurgical intensive care unit: clinical features and outcome. Arch Neurol 2004;61:1090–1094.

[40] Friedman D, Claassen J, Hirsch LJ: Continuous electroencephalogram monitoring in the intensive care unit. Anesth Analg 2009; 109: 506–523.

[41] Sutter R, Kaplan PW, Rüegg S: Independent external validation of the status epilepticus severity score. Crit

Care Med. 2013 Dec;41(12): e475–9. doi: 10.1097/CCM.0b013e31829eca06

[42] Alvarez V, Rossetti AO: Clinical Use of EEG in the ICU: Technical Setting. J Clin Neurophysiol. 2015 Dec;32(6): 481–5. doi: 10.1097/WNP.0000000 000000194.

[43] Akman CI, Micic V, Thompson A, Riviello, JJ Jr: Seizure detection using digital trend analysis: factors affecting utility. Epilepsy Res 2011;93: 66–72.

[44] Williamson CA, Wahlster S, Shafi MM, Westover MB: Sensitivity of compressed spectral arrays for detecting seizures in acutely ill adults. Neurocrit Care 2014;20:32–39.

[45] Fisher R, van Emde Boas W, Blume W, Elger C, Genton P, Lee P, Engel J: "Epileptic seizures and epilepsy: definitions proposed by the International League Against Epilepsy (ILAE) and the International Bureau for Epilepsy (IBE)". Epilepsia. 2005; 46 (4): 470–2. doi:10.1111/j.0013-9580.2005. 66104.x.

[46] Sun T, Guan J: Novel coronavirus and central nervous system. Eur J Neurol 2020 Mar 26, doi: 10.1111/ ene.14227, PMID: 32216009.

[47] Wu Y, Xu X, Chen Z, Duan J, Hashimoto K, Yang L, Liu C, Yang C: Nervous system involvement after infection with COVID-19 and other coronaviruses. Brain Behav Immun 2020 Mar 30, doi: 10.1016/j. bbi.2020.03.031, PMID: 32240762.

[48] Moriguchi T, Harii N, Goto J, Harada D, Sugawara H, Takamino J, Ueno M, Sakata H, Kondo K, Myose N, Nakao A, Takeda M, Haro H, Inoue O, Suzuki-Inoue K, Kubokawa K, Ogihara S, Sasaki T, Kinouchi H, Kojin H, Ito M, Onishi H, Shimizu T, Sasaki Y, Enomoto N, Ishihara H, Furuya S, Yamamoto T, Shimada S: A first case of meningitis/encephalitis associated with SARS-Coronavirus-2. Int J Infect Dis. 2020 May;94:55–58. doi: 10.1016/j.ijid.2020.03.062. Epub 2020 Apr 3. PMID: 32251791; PMCID: PMC7195378.

[49] Mehta P, McAuley DF, Brown M, Sánchez E, Tattersall RS, Manson JJ: COVID-19: consider cytokine storm syndromes and immunosuppression. Lancet 2020, 395, 1033–1034, doi: 10.1016/S0140-6736(20)30628-0.

[50] Vaira LA, Salzano G, Deiana G, De Riu G: Anosmia and ageusia: common findings in COVID-19 patients. Laryngoscope 2020 Apr 1, doi: 10.1002/ lary.28692, PMID: 32237238.

[51] Filatov A, Sharma P, Hindl F, Espinosa PS: Neurological complications of coronavirus (COVID- 19): encephalopathy. Cureus 2020, 12, e7352, doi:10.7759/cureus.7352.

[52] Poyiadji N, Shahin G, Noujaim D, Stone M, Patel S, Griffith B: COVID-19-associated Acute Hemorrhagic Necrotizing Encephalopathy: CT and MRI Features. Radiology 2020 Mar 31, doi: 10.1148/radiol.2020201187, PMID: 32228363.

[53] Chen, C.; Zhang, X.R.; Ju, Z.Y.; He, W.F. Advances in the research of cytokine storm mechanism induced by Corona Virus Disease 2019 and the corresponding immunotherapies. Zhonghua Shao Shang Za Zhi 2020 Mar 1, doi: 10.3760/cma.j. cn501120-20200224-00088, PMID: 32114747.

[54] Li Y, Fu, L, Gonzales DM, Lavi E: Coronavirus neurovirulence correlates with the ability of the virus to induce proinflammatory cytokine signals from astrocytes and microglia. J Virol 2004, 78, 3398–3406, doi: 10.1128/ jvi.78.7.3398-3406.2004, PMID: 15016862.

[55] Kaplan PW, Rossetti AO: EEG patterns and imaging correlations in

encephalopathy: encephalopathy part II. J Clin Neurophysiol 2011, 28, 233–251, doi: 10.1097/WNP.0b013e31821c33a0, PMID: 21633250.

[56] Petrescu A-M, Taussig D, Bouilleret V. Electroencephalogram (EEG) in COVID-19: A systematic retrospective study. Neurophysiol Clin. 2020;50(3):155–165. doi:10.1016/j.neucli.2020.06.001

[57] Pilato MS, Urban A, Alkawadri R, Barot NV, Castellano JF, Rajasekaran V, Bagić AI, Fong-Isariyawongse JS: EEG Findings in Coronavirus Disease. J Clin Neurophysiol. 2020 Jul 1. doi: 10.1097/WNP.0000000000000752. Epub ahead of print. PMID: 32639251.

[58] Scullen T, Keen J, Mathkour M, Dumont AS, Kahn L: Coronavirus 2019 (COVID-19)-Associated Encephalopathies and Cerebrovascular Disease: The New Orleans Experience. World Neurosurg. Published online May 28, 2020. doi:10.1016/j.wneu.2020.05.192

[59] Lindau M, Jelic V, Johansson SE, Andersen C, Wahlund LO, Almkvist O: Quantitative EEG abnormalities and cognitive dysfunctions in frontotemporal dementia and Alzheimer's disease. Dement Geriatr Cogn Disord. 2003;15(2):106–14.

[60] Prichep LS: Quantitative EEG and electromagnetic brain imaging in aging and in the evolution of dementia. Ann N Y Acad Sci. 2007 Feb;1097:156–67

[61] Mizuno T, Takahashi T, Cho RY, Kikuchi M, Murata T, Takahashi K, Wada Y: Assessment of EEG dynamical complexity in Alzheimer's disease using multiscale entropy. Clin Neurophysiol. 2010 Sep;121(9):1438–1446

[62] Abásolo D, Hornero R, Gómez C, García M, López M: Analysis of EEG background activity in Alzheimer's disease patients with Lempel-Ziv complexity and central tendency measure. Med Eng Phys. 2006 May;28(4):315–22.

[63] Abásolo D, Escudero J, Hornero R, Gómez C, Espino P: Approximate entropy and auto mutual information analysis of the electroencephalogram in Alzheimer's disease patients. Med Biol Eng Comput. 2008 Oct;46(10):1019–28.

[64] van der Zande JJ, Gouw AA, van Steenoven I, Scheltens P, Stam CJ, Lemstra AW: EEG Characteristics of Dementia With Lewy Bodies, Alzheimer's Disease and Mixed Pathology. Front Aging Neurosci. 2018 Jul 3;10:190. doi: 10.3389/fnagi.2018.00190. eCollection 2018.

[65] Szelenberger W, Skalski M, Franaszczuk P, Mitraszewski P, Blinowska K: Pharmaco-EEG analysis by means of FFT and FAD. Acta Physiol Pol. 1989 Jul-Aug;40(4):423–30.

[66] Akin M: Comparison of wavelet transform and FFT methods in the analysis of EEG signals. J Med Syst. 2002 Jun;26(3):241–7. doi: 10.1023/a:1015075101937.

[67] Höller Y, Trinka E, Kalss G, Schiepek G, Michaelis R. Correlation of EEG spectra, connectivity, and information theoretical biomarkers with psychological states in the epilepsy monitoring unit - A pilot study: Epilepsy Behav. 2019 Oct;99:106485. doi: 10.1016/j.yebeh.2019.106485. Epub 2019 Sep 4.

[68] Gast H, Schindler K, Rummel C, Herrmann US, Roth C, Hess CW, Mathis J: EEG correlation and power during maintenance of wakefulness test after sleep-deprivation. Clin Neurophysiol. 2011 Oct;122(10):2025–31. doi: 10.1016/j.clinph.2011.03.003. Epub 2011

[69] Kairui Guo, Candra H, Hairong Yu, Huiqi Li, Nguyen HT, Su SW: EEG-

based emotion classification using innovative features and combined SVM and HMM classifier. Annu Int Conf IEEE Eng Med Biol Soc. 2017 Jul;2017: 489–492. doi: 10.1109/EMBC.2017.8036868.

[70] Sanz-García A, Pérez-Romero M, Pastor J, Sola RG, Vega-Zelaya L, Monasterio F, Torrecilla C, Vega G, Pulido P, Ortega G: Potential EEG biomarkers of sedation doses in intensive care patients unveiled by using a machine learning approach. Journal of Neural Engineering, 2019; 16: 026031. https://doi.org/10.1088/1741-2552/ab039f.

[71] Lenartowicz A, Loo SK: Use of EEG to diagnose ADHD. Curr Psychiatry Rep. 2014 Nov;16(11):498. doi: 10.1007/s11920-014-0498-0.

[72] Jiang MJ, Zhang HJ, Li WR, Wu WQ, Huang YM, Xu DM, Qi YY, Qin KY, Zhang L, Zhang JL: Analysis of EEG Lemple-Ziv complexity and correlative aspects before and after treatment of anti-syphilis therapy for neurosyphilis. Neurol Res. 2019 Mar;41 (3):199–203. doi: 10.1080/01616412.2018.1520438.

[73] Sanz-García A, Pérez-Romero M, Pastor J, Sola RG, Vega-Zelaya L, Monasterio F, Torrecilla C, Vega G, Pulido P, Ortega GJ: Identifying causal relationships between EEG activity and intracranial pressure changes in neurocritical care patients. J Neural Eng. 2018 Dec;15(6):066029. doi: 10.1088/1741-2552/aadeea. Epub 2018 Sep 5. PMID: 30181428.

[74] Sanz-García A, Pérez-Romero M, Pastor J, Sola RG, Vega-Zelaya L, Monasterio F, Torrecilla C, Vega G, Pulido P, Ortega G. Potential EEG biomarkers of sedation doses in intensive care patients unveiled by using a machine learning approach. Journal of Neural Engineering, 2019; 16: 026031. https://doi.org/10.1088/1741-2552/ab039f.